Standard Test Procedures and Metrics Development for Automated Guided Vehicle Safety Standards

Roger Bostelman, Will Shackleford, Geraldine Cheok, Richard Norcross
National Institute of Standards and Technology
100 Bureau Drive, Stop 8230
Gaithersburg, MD 20899
(301) 975-3426

roger.bostelman@nist.gov

Abstract
The National Institute of Standards and Technology's Intelligent Systems Division has been researching automated guided vehicle (AGV) control based on advanced two-dimensional (2D) imaging sensors that detect dynamic, standard test pieces representing humans towards improving AGV safety standards. Experiments and results are presented in this paper showing the measurement of dynamic standard test pieces from an automated guided vehicle as compared to ground truth. The experimental results will be used to develop standard test methods and to recommend improved standard stopping distance exception language to AGV standards.

Categories and Subject Descriptors
B.7.0 [Advanced]; C.2.1 [Sensor Networks]

General Terms
Measurement, Performance, Design, Algorithms, Experimentation, Verification.

Keywords
2D/3D imagers, AGV, ANSI/ITSDF B56.5, ground truth

1 Introduction
The Mobile Autonomous Vehicles for Manufacturing (MAVM) Project at the National Institute of Standards and Technology (NIST) is evaluating the performance of advanced sensors as compared to a laser detection and ranging (LADAR) sensor typically used in industry and to ground truth. The American National Standards Institute/Industrial Truck Standards Development Foundation (ANSI/ITSDF) B56.5-2005 Safety Standard for Guided Industrial Vehicles and Automated Functions of Manned Industrial Vehicles "defines the safety requirements relating to the elements of design, operation, and maintenance of powered, not mechanically restrained, unmanned automatic guided industrial vehicles and automated functions of manned industrial vehicles." [1]

 PerMIS'12, March 20-22, 2012, College Park, MD, USA. ACM 978-1-4503-1126-7-3/22/12

NIST recently suggested improvements to the standard including a new test piece, test piece coatings, and non-contact sensor and vehicle performance requirements when detecting static test pieces in the vehicle path. This standard has recently passed ballot at the main committee level. However, the legacy standard still includes an exception for less than the minimum AGV stopping distance. The exception states: "Although the vehicle braking system may be performing correctly and as designed, it cannot be expected to function as designed and specified in para 4.3.1 should an object suddenly appear in the path of the vehicle and within the designed safe stopping distance. Examples include, but are not limited to, an object falling from overhead or a pedestrian stepping into the path of a vehicle at the last instant." Safe stopping distance refers to the distance the AGV travels after a stop command is given and before the AGV contacts an obstacle.

Therefore, the MAVM Project is now performing the second phase of experiments for the ANSI/ITSDF B56.5 standard for dynamic test pieces to once again develop safety standard procedures and metrics. Improved standard language to limit the exception is expected to evolve from the NIST experiments and include discussion of vehicle energy reduction. Initially, NIST must develop an understanding of the typical safety sensor and AGV control characteristics including how accurately the stop function reacts to standard obstacles entering the AGV path. The objectives of the second phase experiments were to:

- Dynamically position a standard test piece in the path of an AGV within the AGV stopping distance, and
- Compare the standard test piece detection point, dynamic test piece path and dynamic AGV path as measured on the vehicle to ground truth to establish a basis for standard test method development

This paper describes the second phase of the AGV experiments and test setup and presents some preliminary results and conclusions. The experimental results will be used to help develop further tests and standard test methods for inclusion in AGV standards, as well as to

develop improved standard stopping distance exception language.

2 Experimental Setup

The parameters investigated in the experiments included the type of test piece, the type of AGV stop (with controlled or e-stop braking), the speeds of the AGV and test piece, the path of the test piece relative to the AGV path, and operation in confined vs. open space. These parameters will be discussed in more detail in this section.

The experimental setup is graphically shown in Figures 1 and 2. Figure 1 shows the basic experimental motion system. The tape switch in Figure 1 triggered the sled motion. Figure 2 shows the test layout with labels describing: the AGV path, the perpendicular and angled test piece paths, sensor locations, and example time intervals showing the test piece crossing the AGV path within the maximum vehicle safe stopping distance.

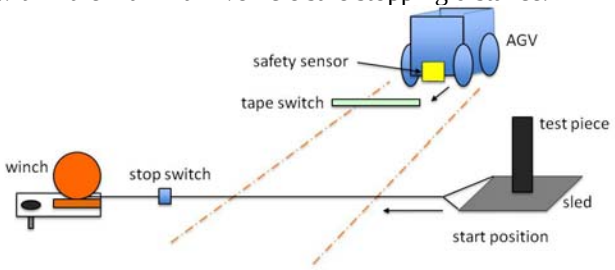

Figure 1 – Test setup showing the AGV, path and test piece sled.

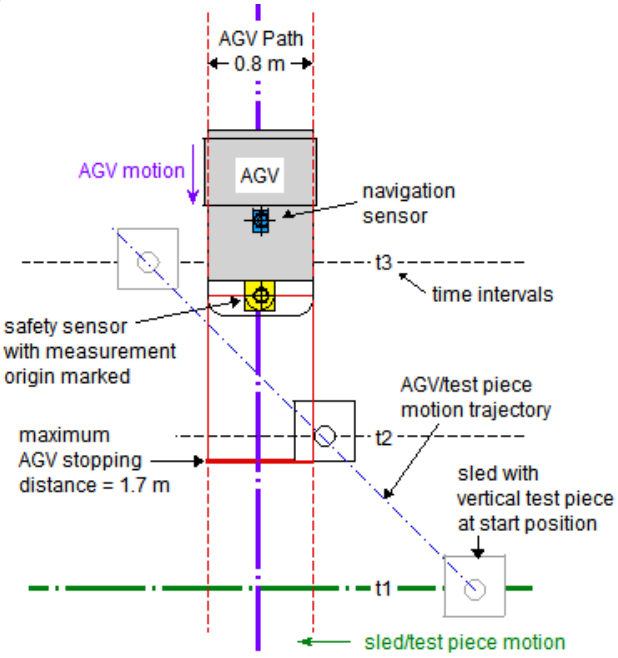

Figure 2 – Top view of test layout with labels describing: the AGV and test piece paths and sensor locations, and example time intervals (t1, t2 and t3) showing the test piece crossing the AGV path within the maximum vehicle stopping distance.

The automated guided vehicle (AGV) used in experiments was equipped with a NIST-built controller, based on the Mobility Open Architecture Simulation and Tools (MOAST) [2] control scheme.

Several sensors were mounted on the NIST AGV which was programmed to move in a straight line to a chosen navigational point. Both two- and three-dimensional (2D and 3D) sensors were used to collect data, including: a color camera, an infrared camera, two different types of 3D light detection and ranging (LIDAR) sensors and a 2D line-scan LADAR sensor. The safety sensor referred to in the discussion below is a 2D LADAR mounted to scan horizontally at a height of 10 cm above the floor. It is a sensor typically used in industry as a non-contact safety sensor for AGVs. The safety sensor's range measurement origin is approximately 70 mm behind the AGV's front foam-on-metal bumper. The data from the 3D imaging sensors will be used in future efforts to research their effectiveness in detecting obstacles, especially overhanging obstacles. For the experiments presented in this paper, the safety sensor data, collected simultaneously with the 3D sensor data, was used for dynamic obstacle detection and for AGV control. The safety sensor was used to detect ground-based obstacles and will later be used as ground truth for the other onboard sensors.

B56.5 states: "The determination of the vehicle's stopping distance … depends on many factors, such as other vehicle and pedestrian traffic, clearances, condition of the floor, and the stability and retention requirements of load(s). The prime consideration is that the braking system in conjunction with the object detection system and the response time of the safety control system shall cause the vehicle to stop prior to impact between the vehicle" and obstacles. Two main types of 'AGV stop' control tests, as described in ANSI/ITSDF B56.5, were performed: controlled braking and low-level emergency stop (e-stop) control.

B56.5 states: "Controlled braking may be provided. Controlled braking is a means for an orderly slowing or stopping of the vehicle." Controlled braking was used to demonstrate continuous AGV control to reduce AGV energy upon detection of an obstacle within the programmed AGV path and at any range detectable from the safety sensor. For example, using controlled braking, the AGV is under continuous control to decelerate to avoid contact with the test piece or other obstacles in the path. The low-level control function is bypassed to consider the effects of only controlled braking during controlled braking tests.

Low-level emergency stop (e-stop) control is required by the standard and is also a function of the NIST AGV which integrates the safety sensor directly into the AGV drive amplifiers. The safety sensor is typically programmed with slow and stop fields. For our tests, only the stop field was programmed and used.

When the safety sensor detected an obstacle in the stop field, the sensor caused the amplifier to be inhibited and the vehicle coasted a maximum distance of 1.7 m (if it was moving at its full speed of 1 m/s), i.e., no additional braking was provided since only stop control was being tested and braking may vary across AGVs due to size, weight, payload, etc. An additional function for the low-level e-stop control is that a timestamp is broadcast through a hardware device to the ground truth system at the instant an obstacle enters the safety sensor stop field. This may prove useful in future analysis.

A thin sled, shown in Figure 3, was designed and built so that it would not be detected by the safety sensor. A modular, laser-based measurement system with 0.01 mm accuracy was used to measure ground truth of the dynamic sled and AGV positions. Eight optical fanning laser transmitters surrounded the AGV/sled test area. Ground truth system receivers were mounted on 1.3 m high posts behind the test piece mounted to a sled Also, two ground truth receivers were mounted to the AGV. (see Figures 3 and 4).

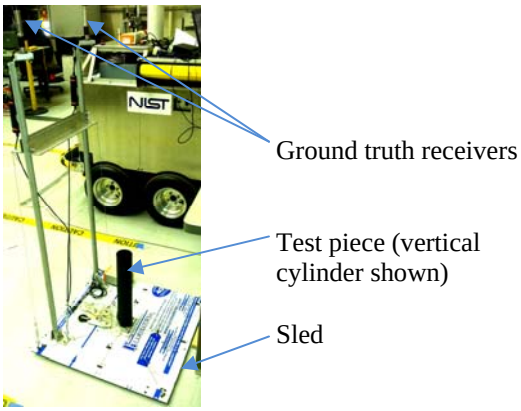

Figure 3 – Sled configuration shown with vertical cylinder test piece.

The sled base measured 64 cm^2 and was made of corrugated plastic between thin aluminum sheets and mounted onto 1.3 cm high teflon strips with their longitudinal axes parallel to the sled motion. The sled was pulled using a winch that began motion when the AGV tripped a tape switch on the floor. Interchangeable test pieces were fixtured to the sled with screws aligning the test piece vertical axis with the sled center point. Test pieces were mounted to the sled so that they entered the AGV path prior to the ground truth sensor posts entering the path.

The tape switch positions were chosen so that the test piece entered and passed through the programmed safety sensor stop zone before the AGV could strike the sled components. The stop zone, used for the low-level, e-stop tests, measured 2 m along the AGV path and 1.3 m perpendicular to the AGV path. The stop zone, used for the controlled braking tests, measured the maximum sensing range along the AGV path by 0.8 m wide. While the sensing range during run-time had no maximum, a 2 m limit was enforced by post-processing. The NIST AGV base measured 0.8 m wide, which sufficed for our tests. However, a roller table extended beyond the 0.8 m width by 0.1 m. This parameter will be included in our future 3D measurement tests and analysisThe AGV had a maximum stopping distance of 1.7 m.

Open and confined spaces (see Figure 4) were another parameter in the NIST experiments. B56.5 states that AGV areas with clearance less than 0.5 m are deemed hazardous and vehicle speed must be reduced.

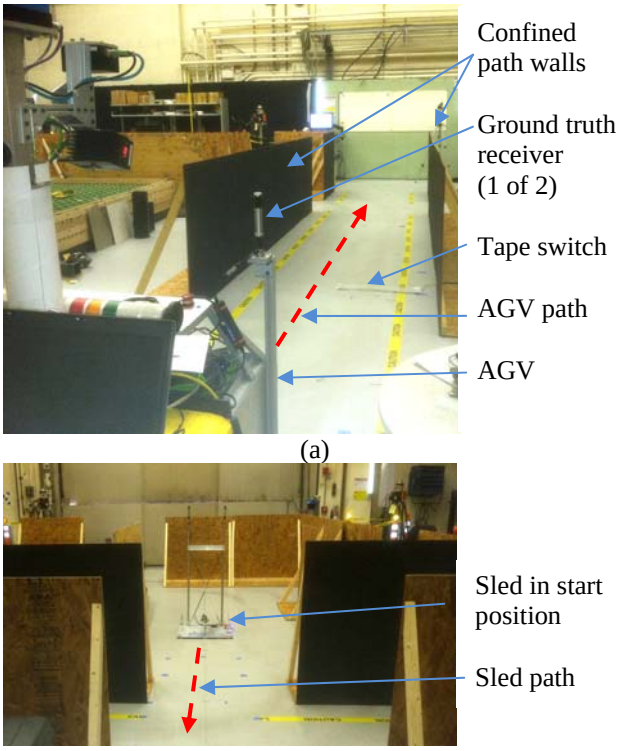

Figure 4 – Confined test course layout showing (a) the AGV paths and (b) the flat plate mounted on the test piece sled and ready to cross the AGV path. The flat plate is mounted with its ½ m square surface facing the AGV path.

Walls representing confined spaces or “hazard zones” were placed 0.15 m beyond the 1.3 m wide stop field making the distance between the walls a total of 1.6 m. Therefore, for confined space tests, the AGV was programmed with a velocity of 0.5 m/s instead of the open-space velocity of 1 m/s. The confined test course was converted to open space by simply removing the black walls and using the same AGV path. The sled path for the confined space tests was perpendicular to the AGV path as shown in Figure 4 (b).

Two cylindrical test pieces were used, as specified in the standard. A vertical cylinder 70 mm in diameter by 400 mm long represented the lower portion of a human leg. A horizontal cylinder 200 mm in diameter by 600 mm long represented the profile of a person lying down. A 0.5 m square flat plate was also used to represent flat, highly reflective materials in a manufacturing environment. The flat plate is part of the draft ANSI/ITSDF B56.5 standard. The cylindrical test pieces were coated with flat black paintwith a 4.6 % reflectivity, measured using a reflectance meter, which is below the maximum 6 % reflectivity allowable by the draft ANSI/ITSDF B56.5 standard. The walls in the confined section of the test course were painted with the same flat black paint to increase the probability of not detecting targets thereby making this a more severe condition.

The ground truth system was initially calibrated and each test piece was modeled so that data for the horizontal cylinder and flat plate reflected the first point that entered the AGV's safety sensor stop field, as shown in Figure 5. However, the vertical cylinder test piece ground truth reference point was on the central axis of the cylinder at mid-height. Since the radius of the cylinder is known, the point on the cylinder detected by the safety sensor can be determined.

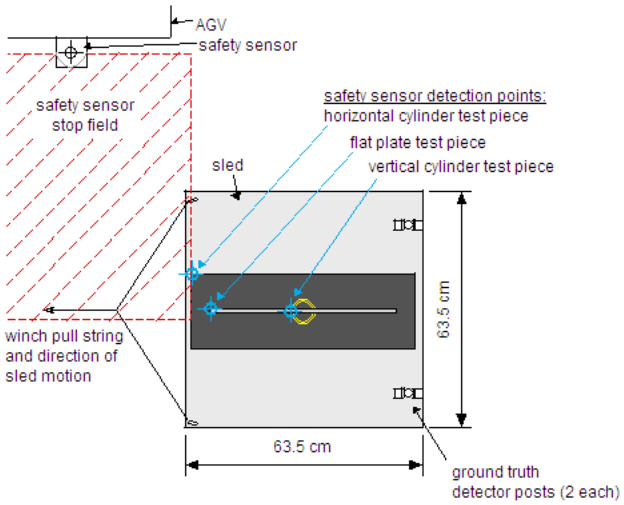

Figure 5 – Top view of initial safety sensor detection points for each test piece as they entered the moving safety sensor stop zone. Only one test piece was mounted on the sled for each test. The vertical cylinder test piece ground truth reference point was at the part center while the other two test pieces matched the points in the figure.

3 Data Collection and Software

The software developed to capture sensor data used the Mobility Open Architecture Simulation and Tools (MOAST) framework [2]. Software was developed using the C++ language for real-time AGV control and for data-collection. Java software was developed for real-time visualization and offline analysis. The Neutral Messaging Language (NML), part of the Real -Time Control Systems (RCS) Library, was used for storing and communicating the data [3]. Three computers were required for data-collection due to bandwidth limitations on each computer. One computer collected data from a high-resolution 3D imager. A second computer collected data from three low-resolution 3D imagers. A third computer controlled the AGV and collected data from the safety sensor, AGV wheel encoders, and navigation system. The Network Time Protocol (NTP) was used to synchronize the clocks on the three computers. [4]

The data collection software also controlled a wireless hardware device used for time synchronization with the ground-truth system. Ground truth was continually collected throughout each test. It was also time-stamped to record detector positions when the hardware device broadcast that the test piece was initially detected, i.e., first entered the stop zone. This information was used to correlate the safety sensor and ground truth detection locations.

4 Experimental Results

Twenty-five tests were completed using the draft ANSI/ITSDF B56.5 standard test pieces. Table 1 shows the tests that were performed (un-shaded cells) and tests that were not performed (shaded cells). The three tests that were not performed were:

- The static AGV (0 m/s) tests. These were performed in previous NIST experiments [6] and led to the initial B56.5 standard changes recently balloted and approved.
- Test piece orientation that is in-line with the AGV path. This test would simulate detection of the edge of the flat plate or horizontal cylinder. The researchers followed the B56.5 safety standard which includes only test methods for test pieces perpendicular to or at a 45° angle to the AGV path.
- A test piece that moves parallel to and towards the AGV in the same lane. This test has not been designed and may require breakaway test pieces and ground truth system components to ensure safety.

To closely model the in-lane tests not performed (explained in the last bullet above), the AGV safety sensor's stop field was programmed to be 1 m wide and within a passing AGV lane. The stop field, in this case, is a programmed safety sensor field that extends into the adjacent lane to sense when a passing test piece is detected. The safety sensor successfully detected the test piece as it paralleled the AGV in an adjacent lane. Results are shown in Tests 23-28.

Experimental results are summarized in Table 2 under the following column headings: test number, AGV velocity, test piece type, safety sensor to test piece range along the AGV path when the test piece first entered the

AGV path, and the difference in test piece location. The last column represents the distance between the location of the test piece as measured by the safety sensor (previous column) and the location as measured by the ground truth instrument. Potential sources of error potentially causing large distance differences are discussed later in this section.

Table 1 – Dynamic experiments performed.

test space	AGV control	AGV velocity	test piece	test piece orientation	test piece movement	test piece velocity	test piece/ AGV sep dist
open	controlled braking	0 - min. speed	vertical cylinder	perp. to path	perp. to and across the path	static	within 2 m
confined	low-level e-stop	50% - confined space speed	horizontal cylinder	45° to path	diag. to and across the path	0.5 mps (slow speed)	beyond 2 m
		100% - open space speed	flat plate	parallel to and in-line with path	parallel to and beside the path	1.0 mps (fast speed)	
					parallel to and in the path		

Seven of the tests listed in Table 2 included the low-level, e-stop control. These tests were used to demonstrate that low-level, e-stop control can reduce the AGV's kinetic energy within its maximum stopping distance and can also control an AGV stop. However, the stop position always occurred beyond the test piece path indicating that a stopped test piece in the path and entering the path within the maximum AGV stopping distance would have been struck. Eighteen controlled braking tests were also performed and demonstrated that once the test piece entered the AGV path within the maximum stopping distance, the AGV could decelerate to a stop without striking a stationary obstacle in the AGV path. For most tests, the tape switch was positioned to allow the test piece to exit the AGV path prior to potential contact and so the AGV slowed to a near stop in the test piece path. After a pause, the AGV began to accelerate again as there were no obstacles in its path. Tests 1, 2, and 12 demonstrated that the vehicle stopped prior to contact with the test piece while the AGV was in both controlled braking and low-level e-stop control modes. During a few tests, not listed in Table 2, the test piece stopped in the path or was struck by the vehicle. To avoid damage to the equipment and sensors, the researchers decided not to stop the test piece in the test path until an experimental setup for this case can be designed and implemented.

Table 2 – Experimental results of safety sensor range uncertainty. Abbreviated column information is as follows:

- *4th column: C = controlled braking and E = low-level, e-stop controlled.*
- *5th column: V = vertical cylinder, H = horizontal cylinder, FP = flat plate, X = 102 mm diameter cylinder.*
- *7th column: the difference in the location where the safety sensor measures the test piece and where the ground truth measures the test piece. This difference is measured along a line parallel to the AGV path.*

Test	Space	AGV/Test Piece Vel (m/s)	Control C or E	Test Piece	Sled Path	Safety Sensor-to-Test Piece Measured Distance (mm)	Diff. in Test Piece Location (mm)
1	Open	1 / 0	E	V	Static	1,702	147
2	"	1 / 0	C	V	Static	1,774	121
3	"	1 / 1	C	V	Perp.	1,205	116
4	"	1 / 1	E	V	Perp.	393	380
6	"	1 / 1	C	H	Perp.	1,158	102
7	"	1 / 1	E	H	Perp.	1,115	114
9	"	1 / 1	E	FP	Perp.	1,005	101
10	"	1 / 1	C	FP	Perp.	772	75
11	Confined	0.5 / 0.5	C	FP	Perp.	490	91
12	"	0.5 / 0	C	FP	Static	517	234
14	"	0.5 / 0.5	E	V	Perp.	460	784
15	"	0.5 / 0.5	C	V	Perp.	506	663
16	"	0.5 / 0.5	E	X	Perp.	380	842
17	"	0.5 / 0.5	E	H	Perp.	527	711
18	"	0.5 / 0.5	C	H	Perp.	1,030	2,240
19	Open	1 / 1	C	V	Angle	1,197	715
20	"	1 / 1	C	V	Angle	1,291	662
21	"	1 / 1	C	FP	Angle	1,409	728
22	"	1 / 1	C	FP	Angle	1,017	747
23	"	1 / 1	C	FP	Parallel	1,556	(281)
24	"	1 / 1	C	FP	Parallel	1,777	(329)
25	"	0.5 / 0.5	C	FP	Parallel	465	(96)
26	"	1 / 1	C	V	Parallel	1,820	(19)
27	"	1 / 1	C	V	Parallel	1,663	43
28	"	1 / 1	C	V	Parallel	506	(25)

Some post-processing was required to determine the safety sensor-to-test piece measured distance reported in the seventh column of Table 2. Post-processing was necessary because the range sensor provides the distance and angle to the test piece, instead of the test piece position when entering the programmed stop zone.

The AGV positions AGV_i (AGV position at time i) and AGV_{i-1} (previous AGV position before time i) are stored in a file and searched based on the timestamp of the obstacle point in another file. Distance was calculated as:

$$\text{distance} = \frac{(AGV_i - AGV_{i-1}) \bullet (TP - AGV_i)}{(AGV_i - AGV_{i-1})}$$

where:

- '$\bullet$' is the 2D XY vector dot product.
- AGV_i and AGV_{i-1} are 2D X and Y vectors.
- TP is the test piece location.

The result provides the distance along the vector that the AGV was travelling just before the obstacle was detected. The ground truth system provided the test piece travel line and was compared to the safety sensor measured location of the test piece.

The distance reported in the last column of Table 2 is the distance between where the safety sensor first detected the test piece and where the ground truth instrument measured the test piece. For the tests reported in this paper, the X-Y plane for the ground truth data corresponded to the lab floor, and the AGV navigation data were in the ground truth coordinate frame. For the tests in which the test piece was stationary, the distance in the last column in Table 2 was the distance between two points: the position of the test piece as measured by the safety sensor and its position as measured by the ground truth system. Since the test piece was stationary, the ground truth system recorded multiple measurements for test piece location and the average location was used in the distance calculation.

For the dynamic tests where the AGV path and the sled path crossed, the steps to calculate this distance in the last column of table 2 were as follows:

1) generate a line to represent the AGV path by best fitting a line through the AGV ground truth XY-data
2) generate a line to represent the sled path by best fitting a line through the sled ground truth XY-data
3) generate a line parallel to the AGV path through Pt. A (see Figure 6 a). Pt. A is the location reported by the safety sensor when it first detects the test piece.
4) Determine the intersection of the line generated in Step 3 with the Sled path. This is Pt. B in Figure 6 a and is the estimated location of the test piece using the data from the ground truth sensor.
5) The distance reported in the last column in Table 2 is the distance *d* between Pt. A and Pt. B in Figure 6 a.

For all of the tests where the path of the AGV and sled crossed, Pt. B was always beyond Pt. A as illustrated in Figure 6 a, i.e., the safety sensor underestimated the distance to the test piece.

For dynamic tests where the AGV and sled paths were parallel, the distance reported in the last column of Table 2 was calculated as follows and as shown in Figure 6 b:

1) generate a line to represent the AGV path by best fitting a line through the AGV ground truth XY-data
2) generate a line to represent the sled path by best fitting a line through the sled ground truth XY-data
3) generate a line, Line 1, through Pt. A perpendicular to the AGV path. Pt. A is the location reported by the safety sensor when it first detects the test piece.
4) create a point (Pt. B in Figure 6 b) on the AGV path that corresponds to the location of the safety sensor, based on safety sensor data, when the target was detected.

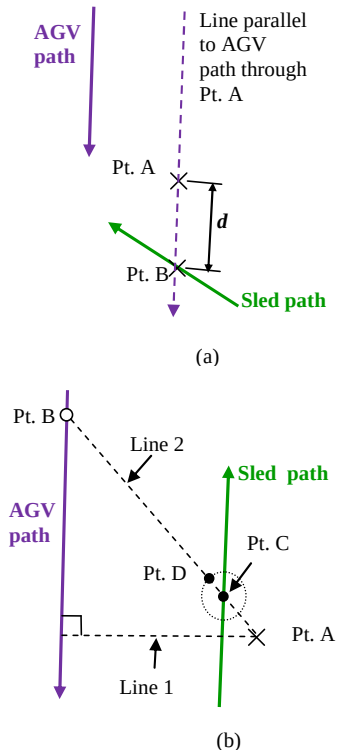

Figure 6. Schematic showing the procedure to determine uncertainty of the location of the test piece (Pt. A) as obtained by the safety sensor for (a) the test piece crossing the AGV path and (b) parallel paths.

5) generate a line through Pt. B and Pt. A.

6a) For Tests 23-25 (flat plate)

1) the intersection of the line from Step 5 and the sled path is Pt. C which is also the point being tracked by the ground truth system
2) the distance reported in last column in Table 2 is the distance from Pt. C to Line 1 along the AGV path and mimicking the same situation as if the test piece was in the same path as the vehicle.

6b) For Tests 26-28 (vertical cylinder)

1) the intersection of the line from Step 5 and the sled path is Pt. C and is the center of the vertical cylinder being tracked by the ground truth system
2) create a point, D, offset from Pt. C by a distance equal to the cylinder radius along Line 2 (Figure 6 b)
3) the distance reported in the last column in Table 2 is the distance from Pt. D to Line 1 along the AGV path and mimicking the same situation as if the test piece was in the same path as the vehicle.

7) In keeping with the sign convention for the crossing paths tests, the distance in the last column in Table 2 is negative if Pt. C or Pt. D was above Line 1 and positive if below Line 1.

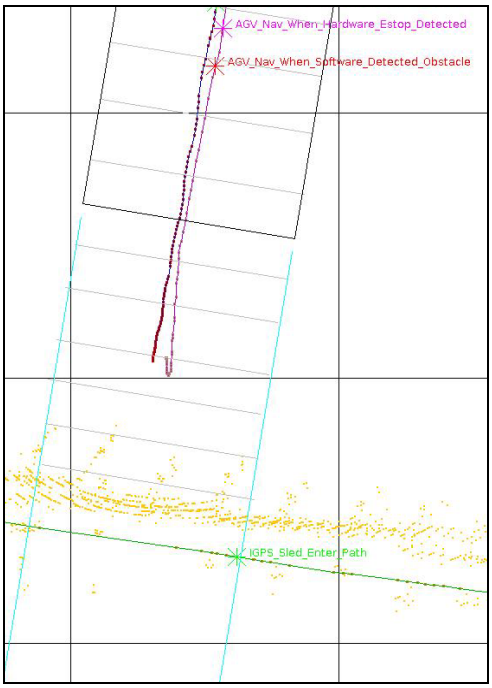

(a)

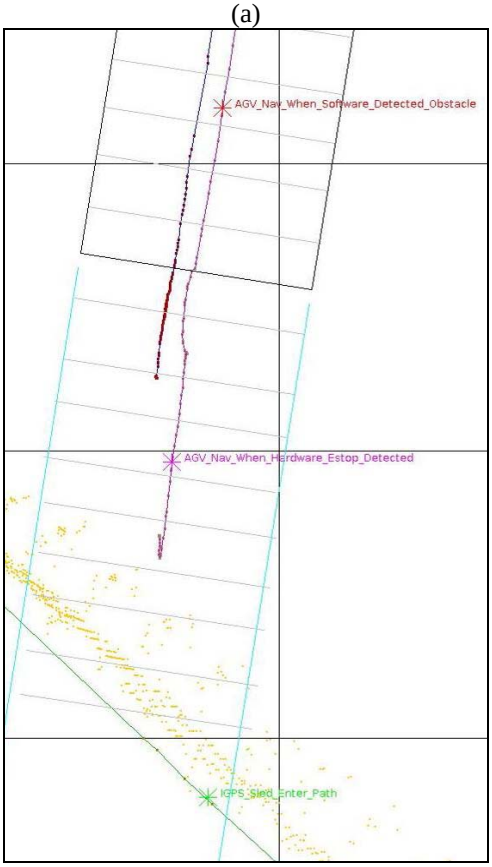

(b)

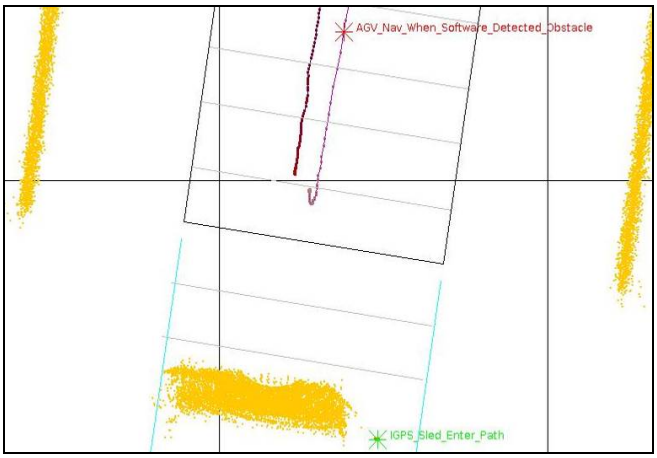

(c)

Figure 7 – Data from (a) Test 7, (b) Test 22, and (c) Test 12 showing the AGV path (gray lines and light green start position), AGV (black rectangle) at the position where it first detected the test piece (yellow crossing vehicle path). In Test 12, yellow lines represent the safety sensor detecting the confined walls and the static test piece in the AGV path. Ground truth of the AGV path centerline (purple) and test piece centerline (dark green) are also shown. Square, black grid lines are spaced at 1 m. Labels on starred points are as follows:

- *Red: AGV Nav when software detected obstacle*
- *Purple: AGV Nav when hardware (i.e., when a researcher pushed an e-stop button)*
- *Green: iGPS sled enter path*

Unlike the crossing path tests, in the parallel path tests (Test 23-28), in five out of the six tests, the safety sensor overestimated the distance to the test piece. This overestimation could result in the AGV hitting the test piece had the test piece been in the AGV path. Also, in the parallel path tests, the ground truth range difference was a lot higher for the Flat Plate compared to the Vertical Cylinder. Further data analysis is required to determine the reason for the large values (values > 500 mm) for the ground truth range differences in Table 2 – especially for Test 18.

Experimental results are shown in Figure 7 for three controlled braking tests (7, 22 and 11). Tests 7 and 22 were open space tests with AGV and test piece velocities set at 1 m/s.

Test 12 was a confined space test with 0.5 m/s AGV velocity and a static test piece. Test pieces used were the black horizontal cylinder for Test 7, black vertical cylinder for Test 22, and highly reflective flat plate for Test 12. Test pieces were perpendicular to the AGV path for Test 7 and 12 and at a 45° angle to the AGV path for Test 22. Test piece orientation was not a factor for Test 22 since it was a vertical cylinder. All tests that included moving test pieces had a test piece-to-AGV safety sensor separation distance of less than the AGV maximum stopping distance. Test 12 shows a point cloud at the test piece and a similar phenomenon resulted in Test 11 (not shown) with skewed data as well. Previous experiments using highly reflective test pieces and detected by light, instead of a laser range scanner as in tests 11 and 12, have

shown similar results. [7] Further analysis is required to interpret these laser-based results.

Potential sources of experimental errors, possibly causing large distance differences between ground truth and the safety sensor-to-test piece distances (i.e., Table 2, column 8), were:

- Poor logging frame rate. Some time gaps were as high as 0.3 s with more common gaps being 0.1 s. The frame rate error could therefore have caused data gaps of 0.15 m to 0.3 m.
- The manufacturer-specified safety system range error and angular resolution were 3 cm and 0.25°, respectively.
- The difference in time between when the navigation sensor and the ground truth sensor recorded the AGV location.
- The Z-value (vertical distance) was ignored for all data. Errors may have occurred if there were undulations in the test space floor that would cause the AGV to slightly tilt and therefore rotate the navigation and safety sensors.

Ground truth tracking of the horizontal cylinder and flat plate are shown in Figure 5. However, the point tracked for the vertical cylinder was the center of the cylinder at mid-height. Therefore, results for this test piece include an offset that varies up to 34 mm depending upon the distance from the safety sensor. The variation in range offset is due to where the test piece surface point is first detected at the angle measured by the safety sensor versus the test piece center point range perpendicular to the AGV path. The offset was used to correlate with the Figure 4 left-most point on the part. The distances in the last column in Table 2 account for this offset. Test 16 included a non- standard, white surface, vertical cylinder test piece with a 102 mm diameter x 1.5 m high with the vertical axis aligned with the sled center. Two similar vertical cylinders were placed on the AGV as well. Test 16 was used to compare two systems that may be used for ground truth measurements. Analysis of this comparative data will be published in a future paper.

5 Conclusions

The NIST Mobile Autonomous Vehicles for Manufacturing Project evaluated automated guided vehicle (AGV) control based on advanced 2D laser imaging safety sensors that can detect dynamic, standard test pieces representing humans. Experiments and results were presented. Both controlled braking and low-level e-stop braking control, as described in ANSI/ITSDF B56.5, were tested. Results showed that both control methods reduce vehicle energy as standard test pieces moved into or were placed in the AGV path and within the AGV's maximum stopping distance. Results also showed that controlled braking provided deceleration to minimize energy that would impact a test piece that appeared within the maximum AGV stopping distance and therefore, could be used to further improve safety near AGV's. Sources of measurement errors were listed after reviewing the results with the largest potential error source being data logging gaps. In most cases, the distance from the safety sensor to the test piece was less than the distance reported by the ground truth system, i.e., the test piece "appeared" closer that it actually was. This is the better case for AGV safety. The experimental results will be used to develop standard test methods and to recommend improved stopping distance exception language in AGV standards. NIST plans to perform more experiments with:

- low reflectivity test pieces beside similar colored walls,
- overhanging obstacles,
- various ground truth measurement systems,
- radio frequency identification (RFID) when used as proximity measurement devices for predicting pedestrian intent to enter the AGV path.

Also, NIST plans to analyze the 3D data for the experiments discussed in this paper and for the future experiments listed.

6 References

[1] ANSI/ITSDF B56.5 -2010 "Safety Standard for Driverless, Automatic Guided Industrial Vehicles and Automated Functions of Manned Industrial Vehicles."

[2] MOAST, http://sourceforge.net/apps/mediawiki/moast/index.php?title=Main_Page

[3] RCS Library, http://www.isd.mel.nist.gov/projects/rcslib/

[4] NTP: The Network Time Protocol, http://www.ntp.org/.

[5] Nikon iGPS, http://www.nikonmetrology.com/large_volume_tracking__positoining/igps/

[6] Bostelman, Roger,; Shackleford, Will, 2009. "Performance Measurements Towards Improved Manufacturing Vehicle Safety," NIST Intelligent Systems Division, PerMIS 09 Proceedings.

[7] Roger Bostelman, Will Shackleford, 2008. "Test Report on Highly Reflective Objects Near the SR3000 Sensor, NIST Internal Report to Consortium CRADA Partners, February 27.